Autofocusing method for lensless digital in-line holographic microscopy with misaligned illumination

Julia Dudek, Mikołaj Rogalski, Julianna Winnik, Piotr Arcab, Piotr Zdańkowski, Maciej Trusiak

Warsaw University of Technology, Institute of Micromechanics and Photonics, 8 Sw. A. Boboli St., 02-525 Warsaw, Poland

Received December 9, 2024; accepted December 27, 2024; published December 31, 2024

Abstract—This study presents a correction method in Lensless Digital In-line Holographic Microscopy accounting for tilted illumination to address challenges caused by misalignments in the optical setup. An autofocusing method is discussed, utilizing a sharpness criterion based on amplitude variance to find both propagation distance and illumination tilt for precise holographic reconstruction of phase objects. The proposed algorithm was rigorously tested under large illumination angles, demonstrating its effectiveness in maintaining high reconstruction quality for demanding imaging scenarios.

Unlike conventional microscopy, where imaging transparent samples is challenging due to their low contrast, Quantitative Phase Imaging (QPI) enables high-contrast visualization of such objects [1]. QPI can precisely quantify refractive index changes and optical thickness variations with nanoscale accuracy. This technique is label-free and highly adaptable, making it a powerful tool for detailed cellular analysis in biomedicine and for studying microstructures in materials science [2]. In this article, we focus on one specific QPI method: Lensless Digital In-line Holographic Microscopy (LDHM) [3]. LDHM offers significant advantages, including simplicity, cost-effectiveness, and a wide field of view (FOV) imaging, all while providing high-quality reconstructions. The absence of lenses in the imaging setup eliminates optical distortions caused by lens aberrations, significantly reduces costs, addresses field of view and depth of field limitations imposed by the numerical aperture of microscope objectives, and enhances the flexibility and adaptability of the system for diverse applications [4-5].

The basic configuration of an LDHM system consists of a coherent light source (typically a laser), a collimating lens (not always required [4-5]), and a sample, all aligned along a system optical axis (Fig. 1). The illuminating beam interacts with the sample, producing both scattered (object beam) and unscattered (reference beam) components. These components interfere, generating a Gabor hologram, which is captured by the CCD camera.

In the reconstruction process, the captured hologram undergoes numerical processing to extract the wavefront information. The hologram is numerically propagated to different planes using algorithms based on the Fresnel [6] or angular spectrum [7] methods. This propagation allows the reconstruction of the optical field at various depths, represented by the parameter z, which denotes the distance from the hologram plane to the reconstructed plane. Determining the correct z parameter is crucial for achieving accurate reconstruction, as incorrect z values lead to blurred or distorted images. This can be done either manually, which is labor-intensive and prone to user errors, or automatically using autofocusing algorithms such as DarkFocus [8], Dubois [9], Tamura [10], or deep learning [11] methods.

In-line holographic systems face the challenge of the twin-image effect, which arises from spatially and spectrally overlapping real and conjugate (virtual) holographic terms [4-5]. As a result, sharply reconstructed real objects (phase and amplitude) are superimposed with double-defocused conjugate ones (twin image), significantly degrading reconstruction quality and making manual focusing even more difficult. Various methods have been proposed to address this issue, such as the Gerchberg-Saxton algorithm [12-13], digital scanning holography [14], the sparsity-based approach [15], or deep learning methods [16-17]. These techniques collectively aim to mitigate the limitations posed by the twin-image effect and improve the overall accuracy and efficiency of holographic imaging.

In a perfectly aligned LDHM system, the autofocusing process should only adjust the propagation distance z. However, achieving perfect alignment of all system elements along an optical axis is inherently challenging. In practice, slight angular misalignment between elements may occur, resulting in the sample being illuminated not along the optical axis (Fig. 1(b)). In this work, we investigate the LDHM reconstruction errors induced by illumination angle misalignment. To correct these errors, we discuss an autofocusing method, which utilizes a sharpness criterion based on amplitude variance to not only find the defocus distance *z* but also to search for the illumination angle (α_x and α_y). We evaluate the proposed algorithm in a system with an introduced arbitrarily large illumination angle (around 40 degrees) to practically amplify the considered angle-dependent effect in LDHM reconstruction.

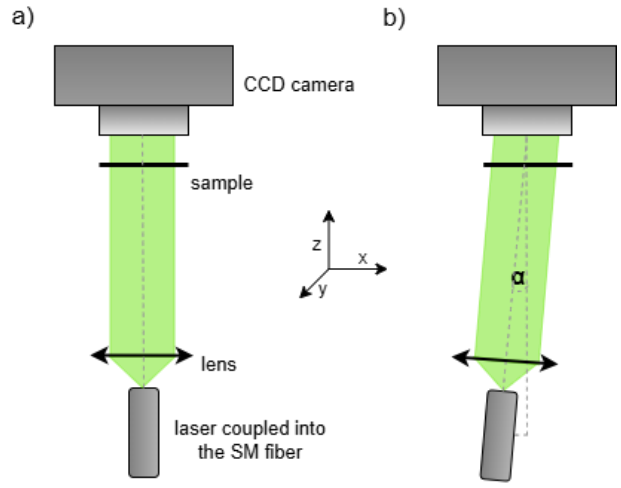

Fig. 1. (a) Experimental setup for a traditional in-line system. (b) Modified setup with integrated angled illumination.

The flow chart of the proposed algorithm is shown in Fig. 2. The algorithm takes as input the angular values (α_x, α_y) and the propagation distance (z) while initializing a sharpness metric M_{best} to infinity. For each combination of α_x, α_y, and z, the hologram is reconstructed, and the algorithm calculates its sharpness using a metric M based on the variance of the amplitude, normalized by its mean. This sharpness metric quantifies the quality of the phase reconstruction, with lower values indicating sharper and more accurate phase results (for phase objects). The calculated metric value is then compared with the current M_{best}. If M is smaller, indicating an improvement in reconstruction quality, M_{best} is updated to the new value. The algorithm iteratively tests all pre-selected combinations of α_x, α_y , and z, repeating the reconstruction and evaluation steps for each parameter set. Once all combinations have been tested, the final hologram is reconstructed using the optimal parameters, producing a high-quality output. Figure 3 presents examples of holographic data reconstruction using manually found z, α_x, and α_y parameters and those determined through the autofocusing algorithm.

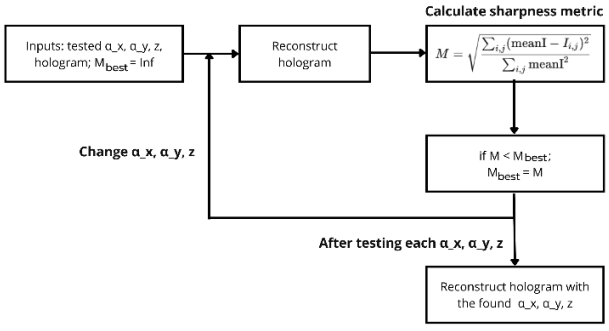

Fig. 2. Autofocusing algorithm based on amplitude variance.

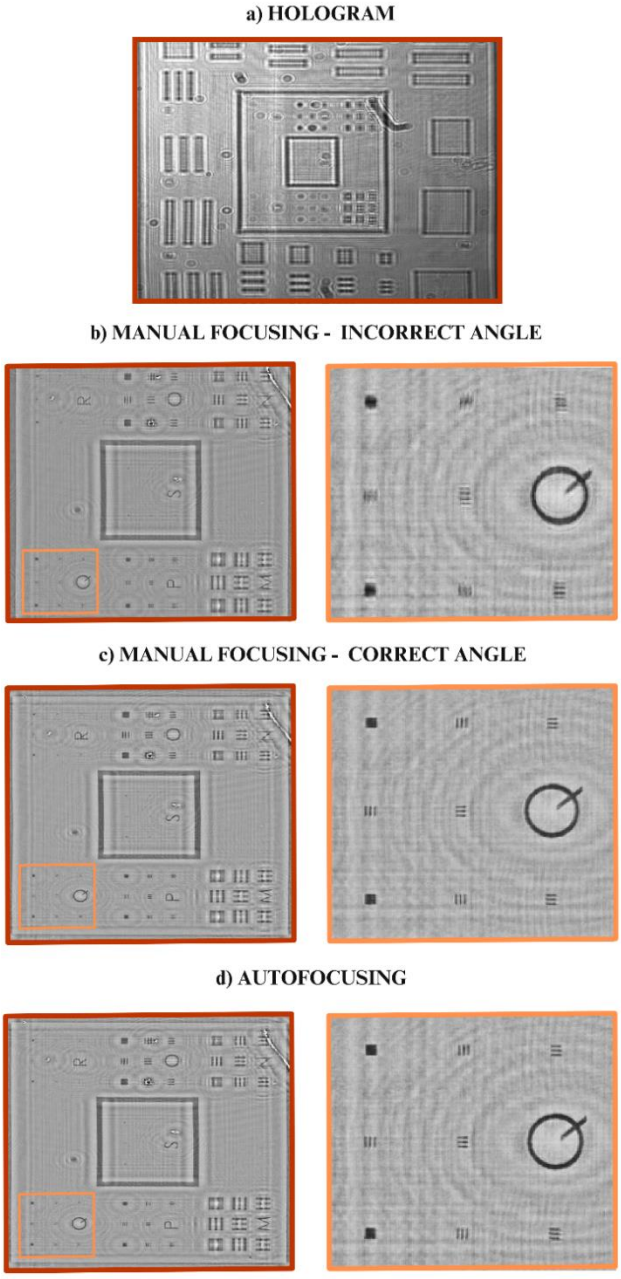

Fig. 3. (a) Example of recorded holographic data. (b) Reconstruction with suboptimal manually set angles (α_x = −39°, α_y: 1.2°, z = 2580 µm) showing poor image quality. (c) Reconstruction with optimal manually set angles (α_x: −41°, α_y: 1.2°, z = 2380 µm) resulting in improved quality. The results demonstrate that with incorrect angles, adjusting the parameter z alone is insufficient to achieve good image quality. (d) Reconstruction using parameters determined through autofocusing (α_x = −41.3°, α_y = 1.5°, z = 2493 µm). Both manual focusing and autofocusing can provide equally high-quality results.

Figure 3(a) shows the acquired full field of view in-line hologram of the resolution phase test target. For the presented data, the optimal angles (α_x = −41°, α_y = 1.2°, z = 2380 µm) were found after manually testing a wide range of input parameters. It is worth highlighting that this

manual process of optimizing three variables was time-consuming and required user expertise. As shown in Fig. 3(c), manually set parameters lead to a sharp and accurate phase reconstruction with minimal distortion. However, when the α_x angle was incorrectly set to −39° (Fig. 3(b)), significant image distortions persisted, even after fine-tuning the z value. This demonstrates the importance of optimizing both angular and distance parameters for high-quality reconstructions. Figure 3(d) presents a reconstruction using parameters determined via the autofocusing algorithm ($\alpha_x = -41.3°$, $\alpha_y = 1.5°$, z = 2493 µm). The results are comparable to the optimal manual settings, highlighting the autofocusing algorithm's efficiency in saving time and ensuring high reconstruction quality under challenging conditions.

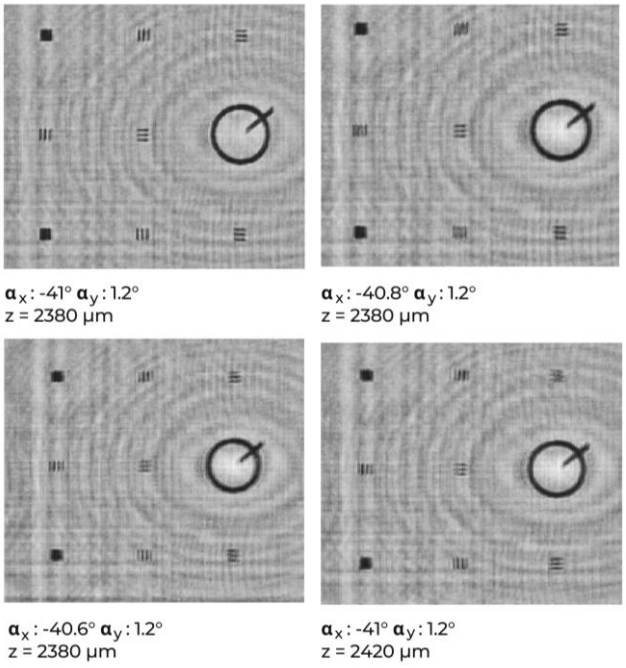

Fig. 4. A comparison of the reconstruction with ideal manually chosen parameters (α_x: −41°, α_y: 1.2°, z = 2380 µm) and reconstructions with slightly varied parameter values demonstrated that the azimuthal angle precision is ±0.2°. The accuracy of the propagation distance is ±40 µm.

The sensitivity of the technique to small parameter variations was analyzed in Fig. 4, emphasizing the critical role of precise settings. Observations indicated that azimuthal angle variations of ±0.2° and propagation distance deviations of ±40 µm caused specific lines of elements from group Q to blur and merge, making them harder to distinguish. This directly impacted the perceived reconstruction quality and highlighted the difficulty of manual focusing, as well as the challenges that autofocusing algorithms must address. As previously mentioned, since autofocusing achieves reconstruction quality comparable to manual focusing, it must also demonstrate a similarly high sensitivity to parameter variations.

The results demonstrate that the proposed algorithm can reliably determine optimal system parameters, achieving reconstruction accuracy comparable to manually selected parameters while eliminating the need for time-intensive adjustments. Tests under varied conditions revealed the robustness of the algorithm, particularly when handling challenging illumination angles, with precise azimuthal and polar angle adjustments ±0.2° and propagation distance tolerances ±40 µm. This automation improves consistency and reproducibility, even in scenarios where small misalignments in the optical setup would otherwise significantly affect image quality.

Studies were funded by Young PW projects granted by Warsaw University of Technology under the program Excellence Initiative: Research University (ID-UB) in POB Photonic Technologies.

Partially funded by the European Union (ERC, NaNoLens, Project 101117392). The views and opinions expressed are, however, those of the author(s) only and do not necessarily reflect those of the European Union or the European Research Council Executive Agency (ERCEA). Neither the European Union nor the granting authority can be held responsible for them.

References

[1] Z. Huang and L. Cao, Light Sci Appl **13**, 145 (2024).
[2] V. Balasubramani, M. Kujawińska, C. Allier, V. Anand, C.-J. Cheng, C. Depeursinge, N. Hai, S. Juodkazis, J. Kalkman, A. Kuś, M. Lee, P.J. Magistretti, P. Marquet, S.H. Ng, J. Rosen, Y.K. Park, and M. Ziemczonok, J. Imaging **7**, 252 (2021).
[3] V. Anand, T. Katkus, D.P. Linklater, E.P. Ivanova, S. Juodkazis, J. Imaging **6**, 99 (2020).
[4] A. Ozcan, E. McLeod, Annual Review of Biomedical Engineering **18**, 77 (2016).
[5] C.J. Potter, Z. Xiong, E. McLeod, Laser Phot. Rev. **18**, 2400197 (2024).
[6] N.N. Evtikhiev, S.N. Starikov, P.A. Cheryomkhin, V.V. Krasnov, V.G. Rodin, **8429**, 84291M (2012).
[7] T. Wu, Y. Yang, H. Wang, H. Chen, H. Zhu, J. Yu, X. Wang, Photonics **11**, 16 (2024).
[8] M. Trusiak, J.-A. Picazo-Bueno, P. Zdankowski, V. Micó, Optics and Lasers in Engineering **134**, 106195 (2020).
[9] F. Dubois, C. Schockaert, N. Callens, C. Yourassowsky, Opt. Express **14**, 5895 (2006).
[10] Y. Zhang, H. Wang, Y. Wu, M. Tamamitsu, A. Ozcan, Opt. Lett. **42**, 3824 (2017).
[11] Z. Ren, Z. Xu, E.Y. Lam, Optica **5**, 337 (2018).
[12] R.W. Gerchberg, W.O. Saxton, Optik **35**, 237 (1972).
[13] J.R. Fienup, Appl. Opt. **21**, 2758 (1982).
[14] T.-C. Poon, T. Kim, G. Indebetouw, B.W. Schilling, M.H. Wu, K. Shinoda, Y. Suzuki, Opt. Lett. **25**, 215 (2000).
[15] Y. Rivenson, Y. Wu, H. Wang, Y. Zhang, A. Feizi, A. Ozcan, Sci. Rep. **6**, 37862 (2016).
[16] M. Rogalski, P. Arcab, L. Stanaszek, V. Micó, C. Zuo, M. Trusiak, Opt. Express **32**, 742 (2024).
[17] Y. Rivenson, Y. Wu, A. Ozcan, Light Sci. Appl. **8**, 85 (2019).

